 doi:10.20944/preprints201808.0353.v1

Article

Hydraulic Features of Flow through Local Non-Submerged Rigid Vegetation in a Y-Shaped Confluence Channel

Xuneng Tong[1], Xiaodong Liu[1]*, Ting Yang[1], Zulin Hua[1], Zian Wang [1], Jingjing Liu [1], Ruoshui Li[1]

1. Key Laboratory of Integrated Regulation and Resource Development on Shallow Lake of Ministry of Education, College of Environment, Hohai University, Nanjing, P.R. China

E-mail: 401046314@qq.com; 1442423532@qq.com; wangzian1996@hotmail.com; 15205168389@163.com; 306407594@qq.com

* Correspondence: E-mail: xdliu@hhu.edu.cn; Tel: +86-139-1597- 4931

Abstract: Vegetation has a significant influence on velocity distribution and turbulent energy in a confluence channel. A laboratory measurement with ADV was used to investigate the flow through a Y-shaped confluence channel partially covered with rigid vegetation on its inner bank. In this study, the flow velocities in cases with and without vegetation were measured by the ADV in a Y-shaped confluence channel. The results clearly show that the existence of non-submerged rigid plants has changed the internal flow structure, that the velocity in the non-vegetated area is greater than in the vegetated area, and that there is a large exchange of mass and momentum between the vegetated and non-vegetated areas. The velocity on both sides is significantly reduced when vegetation is present. In the vicinity of tributaries, due to the presence of vegetation, the high-velocity area moved rapidly to the middle of the non-vegetated area, and the secondary flow phenomenon disappeared. In the mainstream, when vegetation was present, circulation disappeared, and the degree of lateral mixing decreased. The presence of vegetation caused a great change in the internal flow structure and made the flow in non-vegetated areas more intense.

Keywords: Y-shaped confluence channel; non-submerged rigid vegetation; longitudinal velocity; secondary flow; turbulent kinetic energy.

1. Introduction

Channel confluences are a common occurrence in fluvial networks, where significant changes can occur in hydraulics, sediment transport, water environment, and ecology. Many previous studies have concentrated on hydraulic characteristics in channel confluence areas. In terms of confluence patterns, channel confluences fall into two categories: branch inflow main stream confluences and Y-shaped confluences. Due to the complex hydrodynamics in the former type of confluence, the hydrodynamics at channel confluences are characterized by six major regions: flow stagnation, flow deflection, flow separation, maximum flow velocity, gradual flow recovery, and shear layers **Error! Reference source not found.**. In channel confluences, aquatic vegetation is ubiquitous and greatly changes the internal structure of the original flow **Error! Reference source not found.**. Effective water management requires a better understanding of flow structures in vegetated channels. Therefore, it is significant to explore the mechanism of interaction between vegetation and hydraulic flow features.

 doi:10.20944/preprints201808.0353.v1

A number of investigations have examined the influence of vegetation on the hydraulic characteristics of straight open channels. In recent decades, various laboratory experiments have been conducted to study characteristics of open channel flows subject to submerged or emergent vegetation [4–13]. Zhao and Cheng used an array of rigid cylindrical rods to simulate emergent vegetation stems that were subject to unidirectional open channel flows [14]. Nadaoka and Yagi used a two-dimensional shallow-water equation model to simulate a river flow with rigid vegetation [15]. Neary carried out mathematical model tests on water flow with vegetation [16]. Wilson performed laboratory experiments on the effects of two forms (rods or strips) of submerged flexible vegetation on the turbulence structure within the canopy and above the canopy region based on stiffness calculations [17]. Defina and Bixio explored the capability of two mathematical models to predict fully developed one-dimensional open channel flow in the presence of rigid, complex-shaped vegetation with submerged or emergent leaves [18]. Flow resistances in vegetated areas could help resolve a number of conflicting engineering and ecological considerations [19]. The experimental data of Liu have been used to validate a numerical model with double-layered rigid vegetation in a wide Plexiglas recirculating domain [20]. Barrios-Piña's work focused on the effects of vegetation on flow patterns using a mixing-length turbulence model with a three-dimensional eddy-viscosity formulation [21]. Sonnenwald used simultaneous laboratory measurements of transverse and longitudinal dispersion within artificial and real emergent vegetation to predict observed mixing within natural vegetation [22]. In a departure from the straight channel, Xia experimentally investigated the effect of emergent bending riparian-zone vegetation on flow by building up a physical river model [23]. Barrios-Piña, using a hydrodynamic numerical model based on the Reynolds-averaged Navier-Stokes equations, calculated the influence of resistance to water flow as a function of vegetation shear stress [24]. The effect of vegetation on flow structure and flow dispersion in a 180° curved open channel was studied by Huai, who discovered that the primary velocities become much less homogeneous with the presence of vegetation and that the longitudinal dispersion coefficients were much larger than in the non-vegetated case [25]. Stoesser studied the effect of surface roughness on turbulence-driven secondary flow and turbulence statistics by means of a large eddy simulation (LES) method [26]. Pu systematically compared the differences between laboratory-prepared rough bed and water-worked bed open channels in their velocity distributions and three-dimensional (3D) turbulent flow characteristics [27].

Up to now, straight open channel flows with vegetation have attracted enough research attention. However, little attention has been paid to Y-shaped confluences. In this study, a physical model was used to simulate changes of flow state, velocity distribution, turbulence structures, and turbulent kinetic energy caused by vegetation by comparing the results with non-vegetated conditions under the same flow regime.

2. Laboratory Experiments

2.1 Experimental Setup and Measurement Technique

Experiments were conducted in a flat-bottom Plexiglas flume in the Hydraulics Laboratory of Hohai University. Water was pumped into a stilling cistern and then flowed into the flume. The length of the upstream tributaries was 3 m, and the widths were 0.26 m and 0.22 m, respectively.

Preprints (www.preprints.org) | NOT PEER-REVIEWED | Posted: 20 August 2018 doi:10.20944/preprints201808.0353.v1

The length of the downstream main stream was 6 m, and the width was 0.4 m. The convergence angle between the tributaries (the angle between the geometric axes) was 60°. PVC baseboards (1 m × 0.1 m × 0.01 m) were used to cover the entire bottom of the flume. Rigid cylinders were used to simulate rigid vegetation (8 mm diameter, 20 cm height). Figure 1 shows the experimental setup and coordinate system.

The distance measured between the plants was 0.025 m, and the linear spacing was 0.1 m. Vegetation was distributed on both sides of the flume in 2-m-long bands along the two tributaries, and 5-m-long bands along the main stream were planted perpendicularly with the artificial vegetation. In addition, two transition segments and a tailgate were installed to prevent large-scale disturbances from the inlet, thus enabling the development of a quasi-constant water flow by depth. The outlet and the inlet, which were both connected to the tank, enabled continuous recirculation of the steady-state discharges.

Figure 1. Sketch of the experiment.

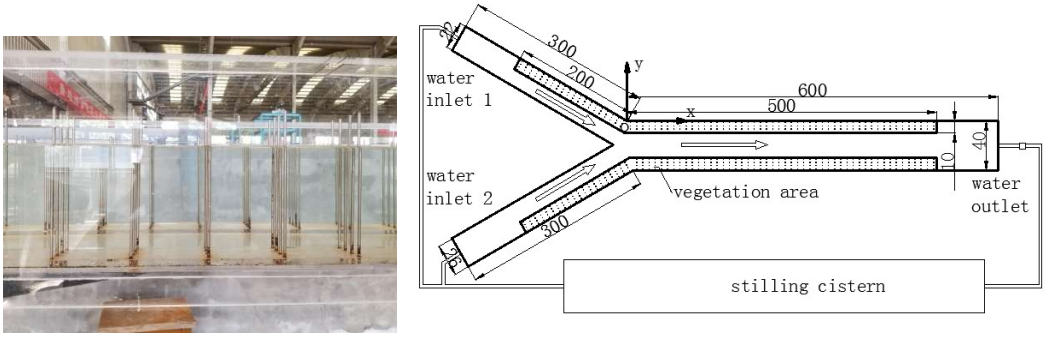

This experiment used two flowmeters to measure the discharge of both tributaries. 3D velocities and velocity fluctuations were measured using a 3D sideways-looking acoustic Doppler velocimeter (ADV) manufactured by SonTek, Inc. (San Diego, CA, USA). The ADV technology is based on the pulse-to-pulse coherent measurement method. The instrument consists of three modules: a measuring probe, a conditioning module, and a processing module [28]. In this study, the ADV was used to sample each measurement point at a frequency of 50 Hz for 30 seconds. The data samples with signal correlations below 80% and signal-to-noise ratios less than 10 were filtered out. The result was that each point had a total of 1500 instantaneous data points, which ensured the adequacy and accuracy of the dataset. To achieve three-dimensional movement control of the ADV, a special regulating device was used to realize three-dimensional free positioning movement of the ADV probe in the test flume. The probe could be easily moved between measurement lines and sections. The ADV was mounted in a wood frame across the center section of the test segment and could be easily moved upstream or downstream, so that all sampling points were vertically aligned. The probe could also channel real-time data to the user's computer through a data acquisition program.

2.2 Test Series Description

To conduct comparative experiments and analyses, both the flume with vegetation and one without vegetation were measured while keeping other conditions unchanged. In this experiment, 18 sections were set up (two sections each on the tributaries and 14 sections on the main stream

Preprints (www.preprints.org) | NOT PEER-REVIEWED | Posted: 20 August 2018 doi:10.20944/preprints201808.0353.v1

after the intersection). The coordinate origin was set at the bottom of the flume, directly below the intersection point of the two tributaries. The x-axis represented the streamwise direction, with $x = 0$ at the leading edge of the patch. The y-axis represented the spanwise direction, with $y = 0$ located on the center line of the flume. The z-axis represented the vertical direction, with $z = 0$ being the channel bed.

Before the intersection, five perpendiculars were established on each section of the tributaries, with each perpendicular having eight measurement points. In other words, there were 40 points in each section. After the intersection, eight perpendiculars were established on each section of the main stream, with each perpendicular having eight measurement points. This means that there were 64 points for each section. There were five survey lines on the two tributaries and seven survey lines on the mainstream. Figures 2a–2c show the sections and the measuring lines.

Figure 2. Sections and measuring lines.

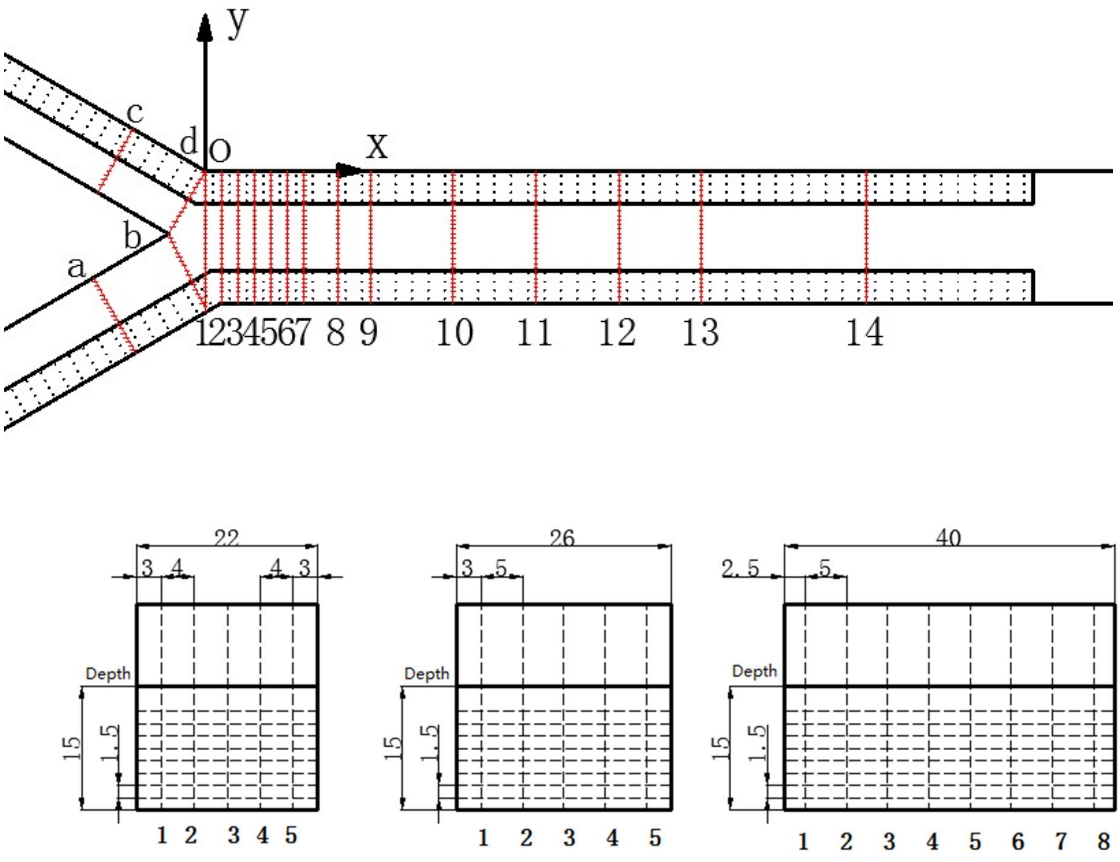

(a) (b) (c)

By comparing the data, seven typical cross sections were chosen for the two vegetation cases to measure flow velocities, and eight vertical measuring lines were arranged in each cross section. The

Preprints (www.preprints.org) | NOT PEER-REVIEWED | Posted: 20 August 2018 doi:10.20944/preprints201808.0353.v1

seven sections were the initial section and intersection of both tributaries and sections 1, 4, and 10 of the main stream. These seven cross sections were defined as cross section (a) (left tributary initial cross section), cross section (b) (left tributary junction cross section), cross section (c) (right tributary initial cross section), cross section (d) (right tributary junction cross section), cross section (e) (main section 1), cross section (f) (main section 4), and cross section (g) (main section 10). All the experimental data were derived from detailed high-resolution measurements on each measuring line.

In the flow characteristics test, the flow rate of the left tributary was $Q_1 = 20\ m^3$/h, and the flow rate of the right tributary was $Q_2 = 20\ m^3$/h. Therefore, the confluence ratio = $Q_1 / Q_2 = 1.0$, and the intersection angle = 60°. The parameters of the experiment, such as the width *b* and the water section depth *h*, are shown in Table 1.

Table 1. Parameters of the experiment.

Element	Q （m^3/h）	b （m）	h （m）	V （m/s）	R_e （10°C）	F_r
Left tributary	20	0.22	0.15	0.17	8168	0.14
Right tributary	20	0.26	0.15	0.14	7584	0.12
Main stream	40	0.4	0.15	0.19	12135	0.16

3. Results and Discussion

3.1 Distribution of streamwise velocity

Li proposed a method to calculate the velocity of a curved open channel with partially non-submerged rigid vegetation by comparing the integral of the longitudinal depth velocity between vegetated and non-vegetated conditions to analyze the changes in the velocity distribution **Error! Reference source not found.**. The streamwise velocities at different water depths in different sections under vegetated conditions were integrated along the depth to obtain the corresponding average streamwise velocity. Due to the limited number of measurement points, the area method of experimental points can be used to circumscribe the area to calculate the experimental measurement points. By comparing the integral of the streamwise depth velocity between vegetated and non-vegetated conditions, the changes in velocity distribution could be analyzed.

Seven typical cross sections were chosen for analysis, consisting of four tributary cross sections and three main cross sections. Figure 3 shows a comparison of depth-averaged streamwise velocities U_{avg} along the Y-shaped confluence channel for vegetated and non-vegetated cases.

Preprints (www.preprints.org) | NOT PEER-REVIEWED | Posted: 20 August 2018 doi:10.20944/preprints201808.0353.v1

Figure 3. Comparison of depth-averaged streamwise velocity transverse distribution between vegetated and non-vegetated cases, where U_{avg} is the depth-averaged streamwise velocity and b is the flume width.

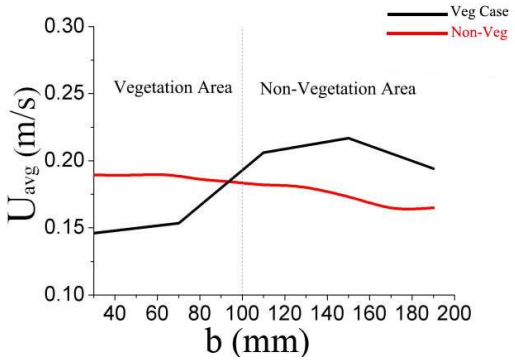

(a) Cross section a

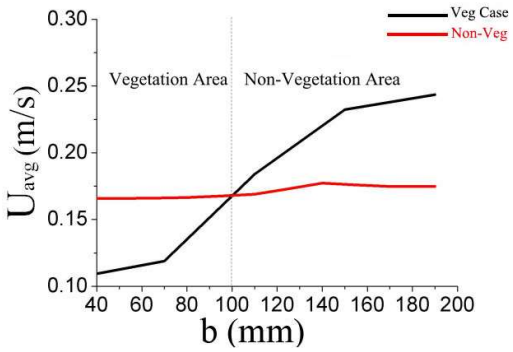

(b) Cross section b

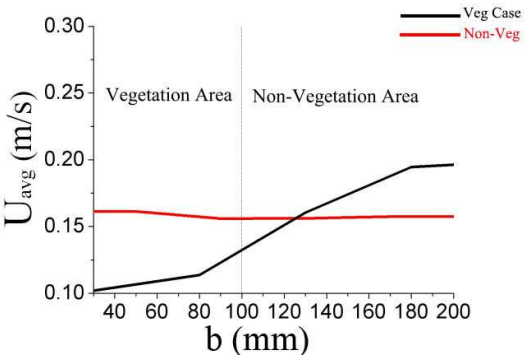

(c) Cross section c

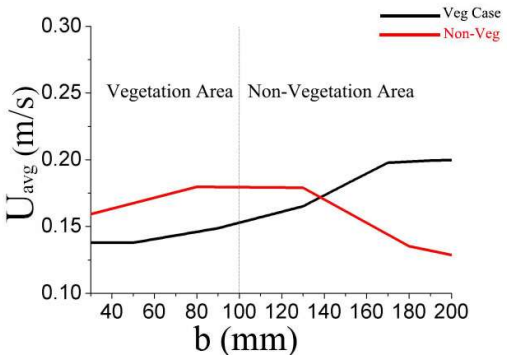

(d) Cross section d

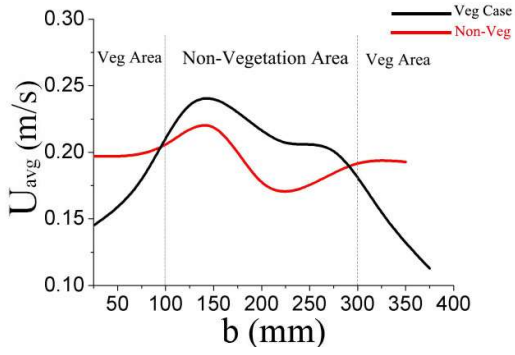

(e) Cross section e

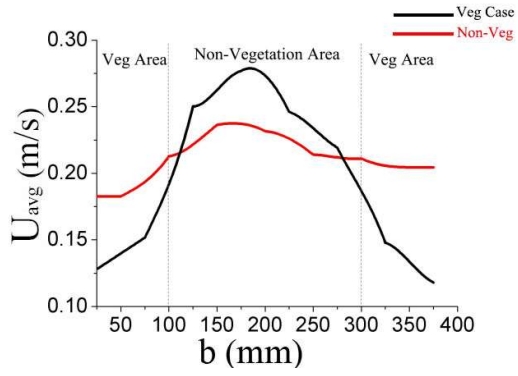

(f) Cross section f

 doi:10.20944/preprints201808.0353.v1

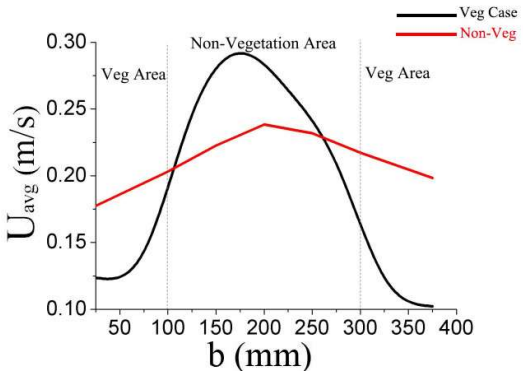

(g) Cross section g

Figure 3 shows that under the retarding effect of vegetation, the depth-averaged streamwise velocities (U_{avg}) in the vegetated region were much lower than in the non-vegetated region. Huai *et al*. [25] reported similarly that the presence of vegetation can decrease flow velocity in vegetated areas. A large velocity gradient was apparent near the junction of the vegetated and non-vegetated areas, indicating that a substantial mass and momentum exchange exists in the junction area.

Figure 3(a–d) also shows a difference in the streamwise velocity distribution between non-vegetated and vegetated cases. The velocities in the vegetated case have a higher gradient than in the non-vegetated case, which can be ascribed to the fact that the retardation caused by vegetation makes the transverse distribution slightly more non-uniform. Along the streamwise direction, the velocities in the vegetated area decreased and those in the non-vegetated area increased when heading downstream. The reason for this may have been that the main circulation in the Y-shaped confluence changed the internal flow structures, and the velocity distribution varied accordingly. In conclusion, under the combined effect of vegetation and the Y-shaped confluence, the streamwise velocities in the vegetated area were much lower than in the non-vegetated area, and the streamwise velocity in non-vegetated areas in the vegetated case increased significantly in the mainstream compared with the non-vegetated case.

Figure 4. Slice diagram of streamwise velocity contour after intersection: (**a**) vegetated case; (**b**) non-vegetated case, where *X*, *Y*, *Z* are the directions of streamwise flow, lateral flow, and vertical flow respectively.

Preprints (www.preprints.org) | NOT PEER-REVIEWED | Posted: 20 August 2018 doi:10.20944/preprints201808.0353.v1

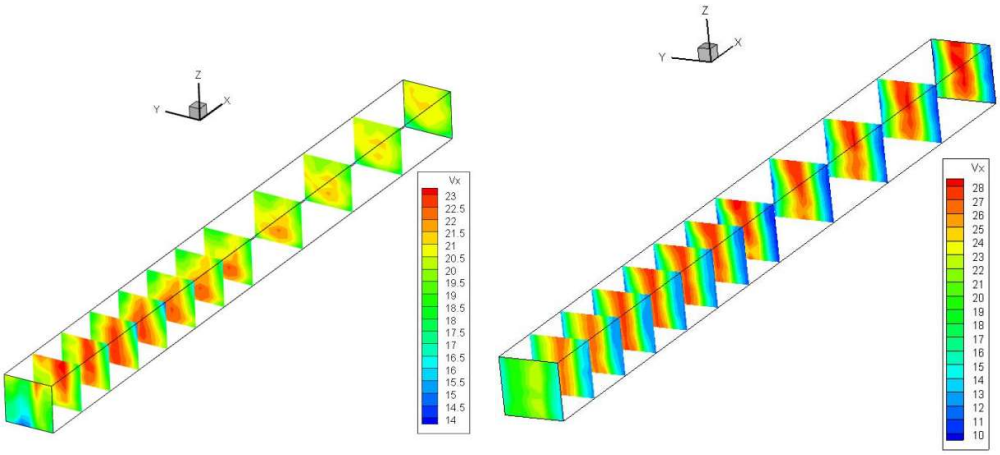

(a) (b)

Three-dimensional flow characteristics were prominent after the intersection. The depth-averaged streamwise velocity distribution was not enough to explain the complex hydrodynamic phenomena. Figure 4 shows a slice diagram of the streamwise velocity contour. Clearly, the flow rate gradient was larger with vegetation than without vegetation, which indicates that the presence of vegetation caused drastic changes in the flow structure of the river. With vegetation, the flow velocity in vegetated zones was less than in non-vegetated zones, indicating that the shear stress of the water flow was increased by planting vegetation and that the water flow rate therefore diminished. It can also be observed that in the absence of vegetation, the longitudinal velocity distribution was polarized in the intersection, with the branch on the left side going downstream having a large flow area, whereas the area close to the right-side tributaries near the bottom was in a low-velocity zone. After mixing, the water velocity in the middle and lower layers was higher, and the near-surface velocity was relatively low.

Downstream of the confluence, a small velocity separation zone appeared on the lateral surface of the left tributary. After vegetation planting, the polarized character of the longitudinal velocity distribution disappeared, the downstream flow velocities in the vegetated areas in the left and right branches obviously diminished, and the flow velocity distribution with depth became insignificant. However, the horizontal flow was significantly layered, the vegetation prevented vertical mixing of fluid, and because of resistance, the velocity near the vegetated side was significantly lowered.

4.2 Secondary Flow Structure

The water mixed energetically in the Y-shaped channels, and three-dimensional flow characteristics were prominent. A single vector or contour map was not enough to explain these complex hydrodynamic phenomena. For ease of explanation, this paper provides and explains a longitudinal velocity contour slice map under the condition Q=1. Each specific section of the

Preprints (www.preprints.org) | NOT PEER-REVIEWED | Posted: 20 August 2018 doi:10.20944/preprints201808.0353.v1

diagram is presented and explained. The study presents a comparative analysis of the flow characteristics of the Y-shaped channels with and without vegetation. The velocity data obtained through the experiments were processed using the Tecplot software. Figure 5 shows the longitudinal velocity distribution with vegetation and Fig. 6 the longitudinal velocity distribution without vegetation.

Figure 5. Comparison of secondary flow structures with vegetation.

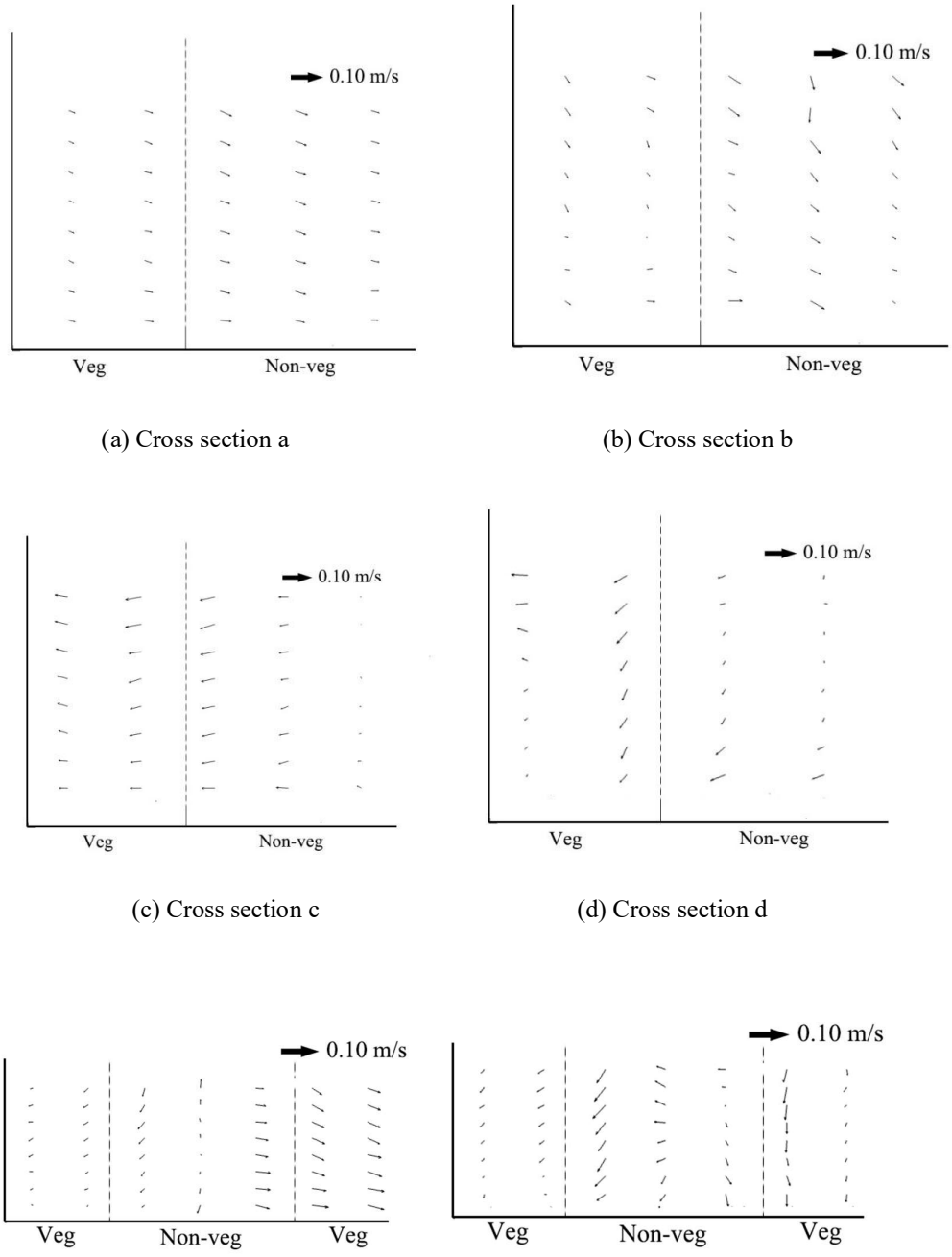

(a) Cross section a

(b) Cross section b

(c) Cross section c

(d) Cross section d

Preprints (www.preprints.org) | NOT PEER-REVIEWED | Posted: 20 August 2018 doi:10.20944/preprints201808.0353.v1

(e) Cross section e (f) Cross section f

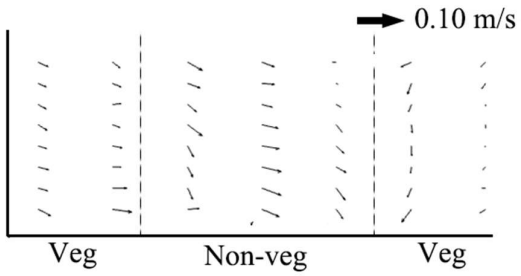

(g) Cross section g

Figure 6. Comparison of secondary flow structures without vegetation.

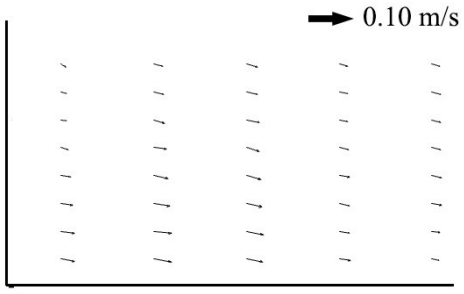

(a) Cross section a

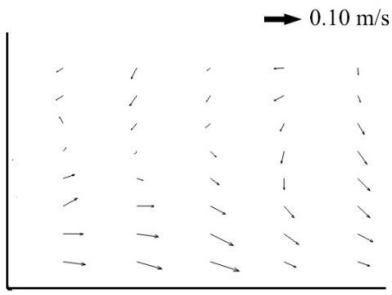

(b) Cross section b

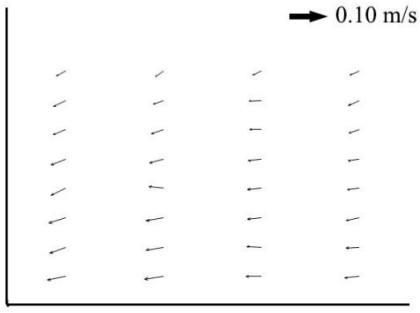

(c) Cross section c

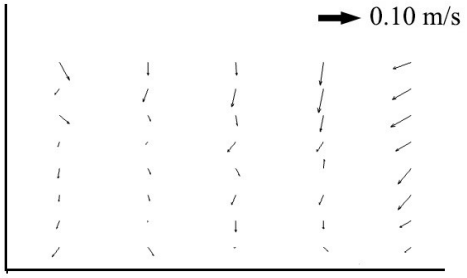

(d) Cross section d

Preprints (www.preprints.org) | NOT PEER-REVIEWED | Posted: 20 August 2018 doi:10.20944/preprints201808.0353.v1

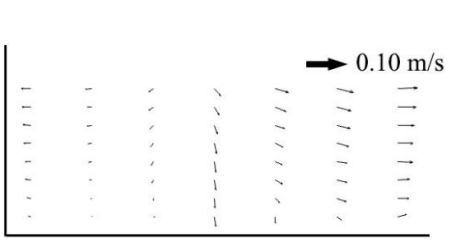

(e) Cross section e

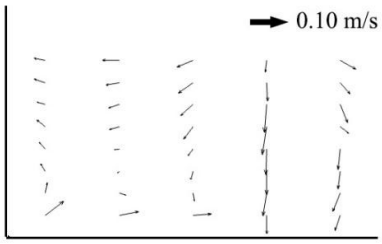

(f) Cross section f

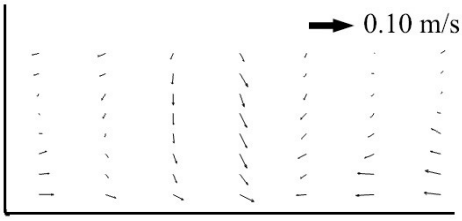

(g) Cross section g

Figures 5 and 6 can be used to compare the experimental results for the confluence of the Y-shaped channels with vegetation (Fig. 5) and without vegetation (Fig. 6). For the mainstream sections (e), (f), and (g), when vegetation was present, the velocity difference in the confluence was more significant. The main section 1 was the confluence cross section; without vegetation, the left velocity was higher, and the right velocity lower. A small clockwise circulation appeared at the bottom of the left side, but there was no circulation in the vegetated case. In addition, with the presence of vegetation, the velocity rapidly became partitioned, with the velocity on both sides decreasing with resistance from vegetation and increasing in the middle. Cross sections (e) and (g) show that the higher-velocity area extended to the center in the non-vegetated case, the bottom of the separation zone became larger, the secondary flow phenomena along the left bank slowly disappeared, and a slight counterclockwise motion appeared in the lower right corner in the mainstream cross section (f). Under the influence of vegetation resistance, the low-velocity zone gradually became wider, the high-speed zone gradually narrowed, the low-speed area on the left changed faster than the low-speed area on the right, and there was no circulation.

4.4 Turbulent Kinetic Energy

The quantitative analysis of turbulent flow is based on measurements of velocity fluctuations at a single point with local non-submerged rigid vegetation and without any vegetation in a Y-shaped confluence channel. In this study, the mean flow velocity components (u, v, and w) and the velocity fluctuation components in turbulent flow (u', v', and w') correspond to the streamwise, lateral, and vertical directions, respectively. Velocity fluctuations can be defined as deviations from the mean

Preprints (www.preprints.org) | NOT PEER-REVIEWED | Posted: 20 August 2018 doi:10.20944/preprints201808.0353.v1

velocity. In general, *turbulent energy* can be considered a measure of turbulence intensity [30]. In this study, the *turbulent kinetic energy* E_k was calculated using Eq. (1), which was proposed by Li [31] and defines E_k as follows in terms of streamwise, lateral, and vertical directions:

$$E_k = \rho(\overline{u'^2}+\overline{v'^2}+\overline{w'^2})/2, \quad (1)$$

where ρ is the density of water and u', v', and w' are the velocity fluctuations of streamwise, lateral, and vertical flow, respectively.

Figures 7 and 8 show the distributions of turbulent energy in different sections with and without vegetation. In the tributary sections, the distribution of turbulent energy is shown along survey lines. In the mainstream sections, seven survey lines are shown.

Figures 6 and 7 show that the turbulent kinetic energy in the tributaries was much smaller with vegetation than without. The maximum value with vegetation was greater than 20 Pa (Figure 7(a–d)), compared to a maximum of less than 15 Pa (Figure 7(a–d)) without vegetation. The turbulent kinetic energy of the vegetated area was less than that of the non-vegetated area, and the turbulent kinetic energy showed a significant increase near the junction of the vegetated and non-vegetated areas. These results indicate that a large velocity gradient was generated at the junction of these areas.

The numerical values of turbulent kinetic energy for each section at different depths were different, but the distribution trends were consistent. After convergence, as shown in Figure 6 (e–g), the turbulent kinetic energy of the non-vegetated area was greater than that of the vegetated area. By comparing Figure 7 (e–g) and Figure 8 (e–g), it is apparent that due to the presence of vegetation, the turbulent kinetic energy of the non-vegetated area in the case without vegetation was significantly greater that in the same location under the case with vegetation. These results indicate that the presence of vegetation caused a great change in the internal flow structure and made the flow in non-vegetated areas more intense.

Figure 7. Turbulent kinetic energy (E_k / Pa) versus relative depth (h/m) with vegetation.

Preprints (www.preprints.org) | NOT PEER-REVIEWED | Posted: 20 August 2018 doi:10.20944/preprints201808.0353.v1

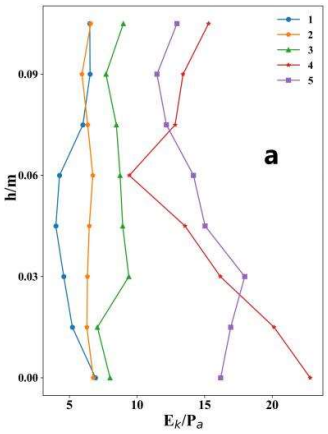

(a) Cross section a

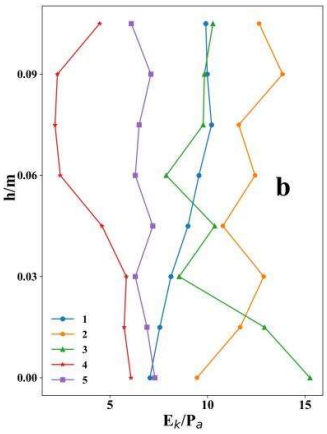

(b) Cross section b

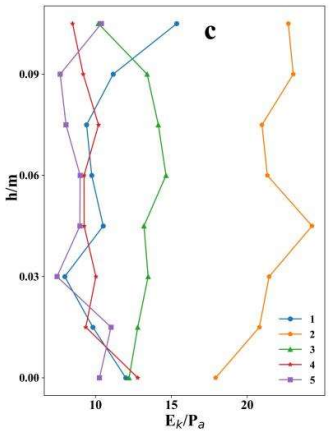

(c) Cross section c

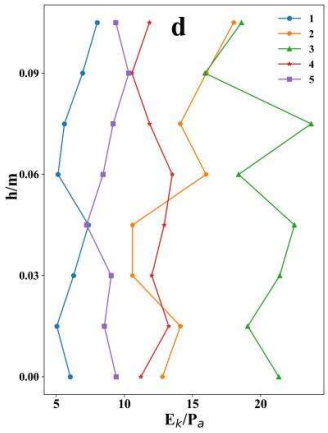

(d) Cross section d

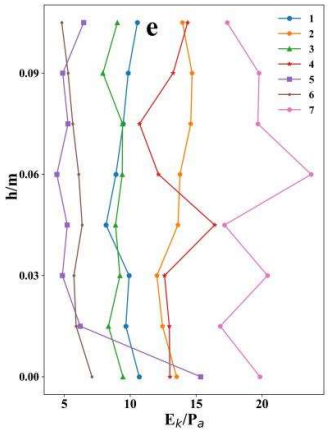

(e) Cross section e

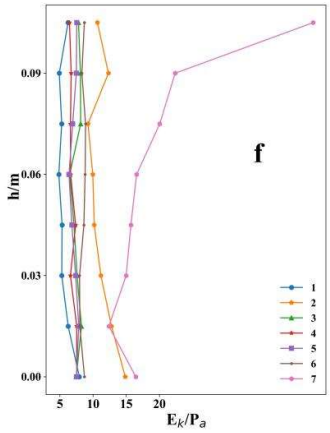

(f) Cross section f

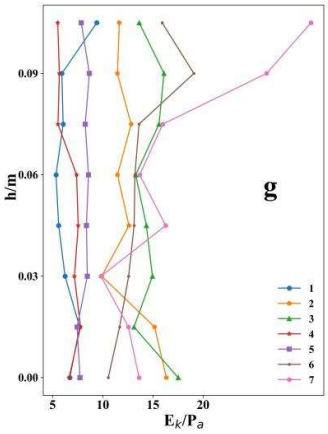

(g) Cross section g

Preprints (www.preprints.org) | NOT PEER-REVIEWED | Posted: 20 August 2018 doi:10.20944/preprints201808.0353.v1

(g) Cross section g

Figure 8. Turbulent kinetic energy (E_k/Pa) versus relative depth (h/m) without vegetation.

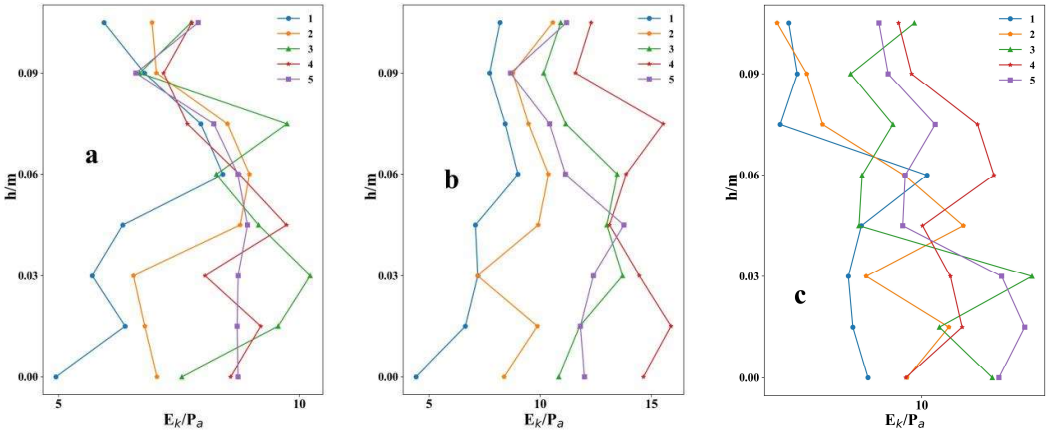

(a) Cross section a (b) Cross section b (c) Cross section c

Preprints (www.preprints.org) | NOT PEER-REVIEWED | Posted: 20 August 2018 doi:10.20944/preprints201808.0353.v1

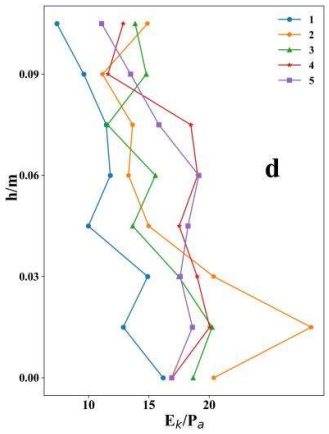

(d) Cross section d

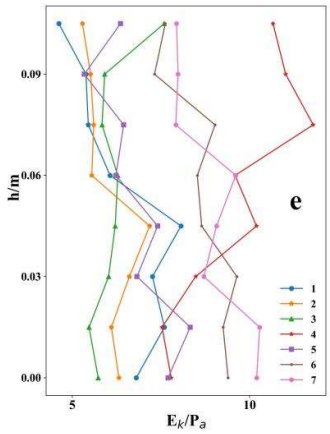

(e) Cross section e

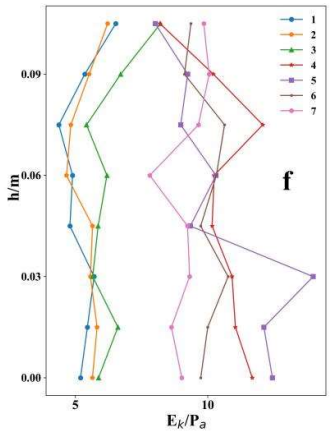

(f) Cross section f

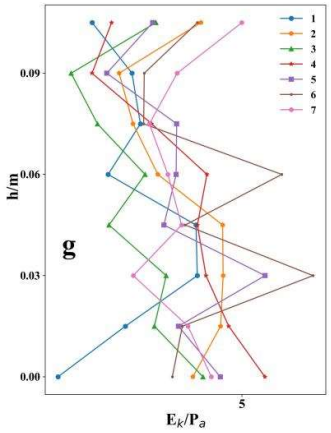

(g) Cross section g

4. Conclusions

This paper has presented an experimental study that explored the effect of local non-submerged rigid vegetation on hydraulic features in a Y-shaped confluence channel. In this study, simulated non-submerged rigid vegetation was arranged into a laboratory Y-shaped confluence flume. An ADV was used to measure the mean velocities and velocity fluctuations.

Due to the presence of vegetation, the flow velocities in the Y-shaped confluence channel were redistributed. Compared with flow without vegetation, the streamwise velocity in the vegetated area was much lower than in the non-vegetated area because of the effect of vegetation. A large exchange of mass and momentum occurred between the vegetated and non-vegetated areas. Under

the combined effect of vegetation and the Y-shaped confluence, the streamwise velocities in vegetated areas were much lower than those in non-vegetated areas, and the streamwise velocity of non-vegetated areas in the mainstream in the case with vegetation increased significantly compared with the case without vegetation.

In the tributaries, due to the presence of vegetation, the high-velocity area moved rapidly to the middle of the channel in non-vegetated areas, and the secondary flow phenomenon disappeared. In the mainstream, when vegetation was introduced, circulation disappeared, and the degree of lateral mixing decreased.

The presence of vegetation brought about great changes in internal flow structure. It causes flow in non-vegetated areas to become more intense, and the turbulent kinetic energy of the tributaries in the cases with vegetation was significantly lower than in the cases without vegetation. At the junction of vegetated and non-vegetated areas, the turbulent energy increased significantly. The turbulent energy of the non-vegetated areas was significantly greater than in the same position in the absence of vegetation.

This work focused on a single type of aquatic plant in the Y-shaped confluence channel. However, rivers actually include several types of plants. Further studies could investigate different vegetation types and different discharges in the Y-shaped channel. This study focused on flume experiments, but further investigations could combine this approach with numerical modeling.

Author Contributions: Conceptualization, Xuneng Tong and Xiaodong Liu; Methodology, Ting Yang; Software, Ruoshui Li; Validation, Jingjing Liu, Zian Wang, and Xuneng Tong; Formal Analysis, Ting Yang; Investigation, Zian Wang; Resources, Zian Wang; Data Curation, Ting Yang; Writing-Original Draft Preparation, Xuneng Tong; Writing-Review & Editing, Xiaodong Liu; Visualization, Xiaodong Liu; Supervision, Xiaodong Liu; Project Administration, Xiaodong Liu; Funding Acquisition, Xiaodong Liu.

Acknowledgments: This research was funded by the National Natural Science Foundation of China (NSFC) (Grant Nos .51479064, 51739002, 51479010, and 51779016) , the National College Students' Innovative Training Project China (Grant No. 201710294031), the National Key Project R& D of China (2016YFC0401702), Jiangsu Province Discipline Construction Funded Projects, Project Funded by the Priority Academic Program Development of Jiangsu Higher Education Institutions (PAPD) and PPZY2015A051.

Conflicts of Interest: The authors declare no conflict of interest.

References

1. Best J L. Sediment transport and bed morphology at river channel confluences. *Sedimentology.* **2010**, 35(3):481-498.
2. Yuan S, Tang H, Xiao Y, et al. Spatial variability of phosphorus adsorption in surface sediment at channel confluences: Field and laboratory experimental evidence. *Journal of Hydro-environment Research.* **2017**, 18:25-36.

3. Merritt D M, Scott M L, Leroy Poff N, et al. Theory, methods and tools for determining environmental flows for riparian vegetation: riparian vegetation-flow response guilds. *Freshwater Biology*. **2010**, 55(1):206-225.

4. Kouwen N, Unny T E, Hill H M. Flow retardance in vegetated channels. *Journal of the Irrigation & Drainage Division*. **1969**, 95:329-342.

5. H. M. Nepf. Drag, turbulence, and diffusion in flow through emergent vegetation. *Water Resources Research*. **1999**, 35(2):1985-1986.

6. Ishikawa Y, Mizuhara K, Ashida S. Effect of density of trees on drag exerted on trees in river channels. *Journal of Forest Research*. **2000**, 5(4):271-279.

7. James C S, Birkhead A L, Jordanova A A, et al. Flow resistance of emergent vegetation. *Journal of Hydraulic Research*. **2004**, 42(4):390-398.

8. JJärvelä, J. Determination of flow resistance caused by non-submerged woody vegetation. *International Journal of River Basin Management*. **2004**, 2(1):61-70.

9. Wilson C A M E, Hoyt J, Schnauder I. Impact of Foliage on the Drag Force of Vegetation in Aquatic Flows. *Journal of Hydraulic Engineering*. **2008**, 134(7):885-891.

10. Wu, F.-S. Characteristics of Flow Resistance in Open Channels with Non-submerged rigid vegetation. *J. Hydrodyn*. **2008**, 20(2), 239–245.

11. Kothyari U C, KenjirouHayashi, HaruyukiHashimoto. Drag coefficient of unsubmerged rigid vegetation stems in open channel flows. *Journal of Hydraulic Research*. **2009**, 47(6):691-699.

12. Wonjun Yang, Sung-Uk Choi. A two-layer approach for depth-limited open-channel flows with submerged vegetation. *Journal of Hydraulic Research*. **2010**, 48(4):466-475.

13. Cheng N S, Nguyen H T. Hydraulic Radius for Evaluating Resistance Induced by Simulated Emergent Vegetation in Open-Channel Flows. *Journal of Hydraulic Engineering*. **2011**, 137(137):995-1004.

14. Zhao K, Cheng N S, Wang X, et al. Measurements of Fluctuation in Drag Acting on Rigid Cylinder Array in Open Channel Flow. *Journal of Hydraulic Engineering*. **2014**, 140(1):48-55.

15. Nadaoka K. Shallow-water turbulence modeling and horizontal large-eddy computation of river flow[J]. *Journal of Hydraulic Engineering*. **1998**, 124(5):493-500.

16. Neary V S. Numerical Solution of Fully Developed Flow with Vegetative Resistance. *Journal of Engineering Mechanics*. **2003**, 129(5):558-563.

17. Catherine Wilson, A Batemann Pinzen, P D Bates, et al. Open Channel Flow through Different Forms of Submerged Flexible Vegetation. *Journal of Hydraulic Engineering*. **2006**, 129(11):750-750.

18. Defina, A.; Bixio, A.C. Mean flow and turbulence in vegetated open channel flow. *Water Resour. Res.* **2005**, 41, W07006.

19. Järvelä,J, Aberle.J, Dittrich.A; Schnauder.I, Rauch, H.P. Flow–Vegetation–Sediment Interaction: Research Challenges. In Proceedings of International Conference River Flow, London,UK, 2006; Ferreira, R.M.L.Alves, E.C.T.L.Leal, J.G.A.B.Cardoso, A.H.Eds.Taylor & Francis:London, UK, 6-8 September 2006. Volume 2, pp. 2017–2020.

20. Liu D, Diplas P, Hodges C C, et al. Hydrodynamics of flow through double layer rigid vegetation. *Geomorphology*. **2010**, 116(3):286-296.

21. Hector Barrios-Piña, Hermilo Ramírez-León, Clemente Rodríguez-Cuevas, Carlos Couder-Castañeda. Multilayer Numerical Modeling of Flows through Vegetation Using a Mixing-Length Turbulence Model. *Water*. **2014**, 6, 2084-2103.

22. F. Sonnenwald, J. R. Hart,P. West. Transverse and longitudinal mixing in real emergentvegetation at low velocities. *Water Resour. Res*. **2017**, 53, 961–978.

23. Xia Jihong, Nehal, Launia. Hydraulic Features of Flow through Emergent Bending Aquatic Vegetation in the Riparian Zone. *Water*. **2013**, 5, 2080-2093.

24. Hector Barrios-Piña, Hermilo Ramírez-León, Clemente Rodríguez-Cuevas, Carlos Couder-Castañeda. Multilayer Numerical Modeling of Flows through Vegetation Using a Mixing-Length Turbulence Model. *Water*. **2014**, 6, 2084-2103.

25. HUAI Wen-xin, LI Cheng-guang, ZENG Yu-hong.Curved open channel flow on vegetation roughened inner bank. *Journal of Hydrodynamics*. **2012**, 24 (1) :124-129.

26. Jaan Hui Pu, Jiahua Wei, Yuefei Huang. Velocity Distribution and 3D Turbulence Characteristic Analys for Flow over Water-Worked. *Water*. **2017**.9.668.

27. Thorsten Stoesser, Richard McSherry, Bruno FragaRough. Secondary Currents and Turbulence over a Non-Uniformly Roughened Open-Channel Bed. *Water*. **2015**,7,4896-4913s.

28. Yagci, O.; Tschiesche, U.; Kabdasli, M.S. The role of different forms of natural riparian vegetation on turbulence and kinetic energy characteristics. Adv. *Water Resour*. **2010**, 33, 601–614.

29. Cheng-Guang L I, Xue W Y, Huai W X. Effect of vegetation on flow structure and dispersion in strongly curved channels. *Journal of Hydrodynamics*. **2015**, 27(2):286-291.

30. Li Kun-fang, WANG Dan, YANG Ke-jun, ZHU Ming-ming. Distribution of Turbulent Energy in Open Channel with Vegetation Patch. *Water Resources and Power*. 1000-7709 (**2017**) 02-0116-03.